Supporting Information

Environmental chemistry response of beryllium to diverse soil-solution conditions at a waste disposal site

Md. Rashidul Islam[a,b]*; Peter Sanderson[a,b]; Mathew P. Johansen[c]; Timothy E. Payne[c]; Ravi Naidu[a,b]**

[a]Global Centre for Environmental Remediation (GCER), College of Engineering, Science and Environment; The University of Newcastle, University Drive, Callaghan Campus, NSW 2308, Australia.

[b]CRC for Contamination Assessment and Remediation of the Environment (CARE), The University of Newcastle, University Drive, Callaghan Campus, NSW 2308, Australia.

[c]Australian Nuclear Science and Technology Organisation (ANSTO), Lucas Heights, NSW 2234, Australia.

Corresponding authors (* and **): Global Centre for Environmental Remediation, and CRC for Contamination Assessment and Remediation of the Environment (CARE), The University of Newcastle, University Drive, Callaghan Campus, NSW 2308, Australia

Contacts: ravi.naidu@newcastle.edu.au (+61 2 4913 8705) and

md.rashidul.islam@uon.edu.au (+61470219676)

Method

Study site

The study site referred to as Little Forest Legacy Site (LFLS) is located near Lucas Heights on the southern periphery of Sydney. The site for the disposals was selected in a small area of a clay/shale lens (only a few hundred metres across), whereas the surrounding area and the formation underlying the site are predominantly sandstone [1, 2]. There are 79 waste trenches covered by 1 m of the local clay soil at the centre of the site. The waste trenches are nominally 25 m long, 0.6 m wide, 3 m deep, and 2.7 m apart. Adjacent to the western edge of the LFLS is a former landfill, and there are other nearby legacy waste disposal sites for industrial chemicals and sewage effluent, which could influence background levels of Be and other contaminants. An industrial liquid waste disposal site is to the north-west of the LFLS. It was used to dispose of grease, paints, solvents, and tannery wastes, as well as other specific hazardous industrial chemicals such as dioxin-contaminated material and residues from herbicide production [3]. There may be a mixing of contaminant plumes from the various waste disposal sites, including the LFLS [2, 4].

The disposed waste materials at LFLS existed in the form of a range of solids, liquids, and sludges, which originated from the operation of the research facility and included waste drums, chemicals, disused equipment, laboratory trash, and radioactive waste (including various radionuclides ranging from tritium, fission products and Co-60, to actinides such as U-233 and Pu). Of particular relevance to the current study is the disposal of approximately ~1070 kg of Be wastes, which arose from research into the fabrication of nuclear fuel containing Be [5]. However, at the time of disposal in the 1960s, it was recognised that potential Be releases posed one of the greatest risks to the local environment due to its high toxicity [1]. Nearly 800 drums of sludge wastes (each 44 gallon /198 litre) arising from research activities were also disposed of at the site, comprising a major component of the buried wastes, and also comprising

a potential source of Be. It was reported by the AAEC that some of the drums were badly deteriorated prior to disposal, and were difficult to remove from the area in that condition [6]. In the period since burials concluded, subsidence above the trenches has been reported, due to voids developing in the waste caused by further deterioration of disposed containers and objects [3]. The subsidence has been managed by adding additional soil- sourced from the local area- to the ground surface.

Intense rainfall events at the site result in periodic infiltration and wetting that can saturate the waste trenches (bathtub effect), which influences the mobility of contaminants [4]. Surface water runoff from the LFLS site could affect a local creek known as 'Turtle Creek', which is hydrologically down gradient, and subsequently impact other nearby creeks and rivers such as Barden's Creek and Mill Creek. As well, the Barden Ridge suburb is 2.5 km to the east, while the suburb of Menai Ridge is 3 km to the north of the study area, and potential Be releases may pose one of the greatest risks to the local environment due to its high toxicity.

Physicochemical properties of LFLS soil

The basic physicochemical properties of LFLS soil (0-10 cm depth, <2 mm) include the following: pH, electrical conductivity (EC), cation exchange capacity (CEC, by compulsive exchange method), soil texture (hydrometer method), soil total carbon [STC, by carbon-nitrogen-sulphur (CNS) analyser], soil organic matter (SOM), Brunauer-Emmett-Teller (BET) surface area (nitrogen gas adsorption-desorption using Micromeritics Tristar II 3020) [7, 8] were measured following standard methodology. Water holding capacity (WHC) was determined using soaking of soil with Milli-Q water followed by the gravimetric water content method [9]. XRD (Bruker D8 advanced X-ray powder diffractometer) for mineralogical study; Scanning Electron Microscope (SEM, Zeiss Sigma VP FESEM, Germany) and Transition Electron Microscope (TEM, JEOL LaB6 2100, Japan) were used for surface morphology.

Results and discussion

Table S1 The average value of different physicochemical properties of LFLS soil [7].

Parameter	Average value ± SD
pH-water (1:5)	6.06±0.13
pH-$CaCl_2$ (1:5)	4.60±0.17
CEC (cmol/kg)	5.41±0.40
% Sand	55.7±2.3
% Clay	12.7±1.2
% Silt	31.8±2.3
% Nitrogen (N)	0.21±0.06
% Sulphur (S)	0.02±0.005
% STC	4.27±0.70
% SOC	3.70±0.44
% SOM	6.37±0.75
WHC (%)	56
pH_{zpc}	5.24
IEP	2.10

Table S2 Langmuir and Freundlich desorption isotherm parameters of Be at different temperatures and desorption cycles.

	Langmuir model				Freundlich model			
Temperatures	K_{Ld} (L/mg)	q_{mLd} (mg/g)	X^2	R^2	K_{Fd} (mg/L)	n_d	X^2	R^2
318K C1	4.18 ± 0.34	0.953 ± 0.05	2.6E-05	0.9992	1.45 ± 0.12	1.36 ± 0.08	2.1E-04	0.9936
318K C2	5.81 ± 0.73	0.890 ± 0.07	7.3E-05	0.9978	1.59 ± 0.17	1.41 ± 0.10	3.0E-04	0.9910
318K C3	6.57 ± 0.72	0.893 ± 0.06	5.4E-05	0.9984	1.74 ± 0.17	1.41 ± 0.08	2.1E-04	0.9938
318K C4	6.83 ± 0.70	0.866± 0.05	5.1E-05	0.9985	1.71 ± 0.20	1.42 ± 0.10	3.5E-04	0.9898
308K C1	5.38 ± 0.57	0.809 ± 0.05	6.3E-05	0.9981	1.26 ± 0.14	1.47 ± 0.12	4.3E-04	0.9869
308K C2	7.23 ± 0.39	0.778 ± 0.02	1.6E-05	0.9995	1.41 ± 0.14	1.51 ± 0.10	3.1E-04	0.9908
308K C3	8.61± 0.47	0.772 ± 0.02	1.7E-05	0.9995	1.59 ± 0.17	1.49 ± 0.10	3.1E-04	0.9906
308K C4	7.81 ± 0.38	0.786 ± 0.02	1.3E-05	0.9996	1.53 ± 0.16	1.49 ± 0.10	2.9E-04	0.9912
298K C1	4.89 ± 0.51	0.851 ± 0.05	4.2E-05	0.9987	1.32 ± 0.05	1.43 ± 0.04	4.5E-05	0.9986
298K C2	6.57 ± 0.88	0.795 ± 0.06	7.8E-05	0.9976	1.41 ± 0.08	1.48 ± 0.05	7.8E-05	0.9976
298K C3	7.58± 0.93	0.775 ± 0.05	6.8E-05	0.9979	1.48 ± 0.08	1.50 ± 0.05	6.5E-05	0.9980
298K C4	8.10 ± 1.05	0.730 ± 0.05	8.3E-05	0.9974	1.38 ± 0.07	1.54 ± 0.06	7.7E-05	0.9976
288K C1	1.57 ± 0.52	1.611 ± 0.42	1.1E-04	0.9966	1.46 ± 0.05	1.21 ± 0.03	2.7E-05	0.9991
288K C2	2.22 ± 0.85	1.370 ± 0.39	1.8E-04	0.9941	1.55 ± 0.10	1.24 ± 0.05	7.4E-05	0.9976
288K C3	2.90 ± 0.89	1.237 ± 0.27	1.5E-04	0.9952	1.66 ± 0.09	1.27 ± 0.04	5.1E-05	0.9984
288K C4	7.61 ± 1.00	0.693 ± 0.05	9.1E-05	0.9971	1.19 ± 0.06	1.58 ± 0.06	8.9E-05	0.9972

Note: K_{Ld}, and q_{mLd} are the Langmuir constant, and sorption maximum taking into account the desorption of Be in each desorption cycle; K_{Fd}, and n_d are the Freundlich constants, and sorption intensity where each desorption cycle is considered; X^2= chi-square; R^2= linear regression coefficient.

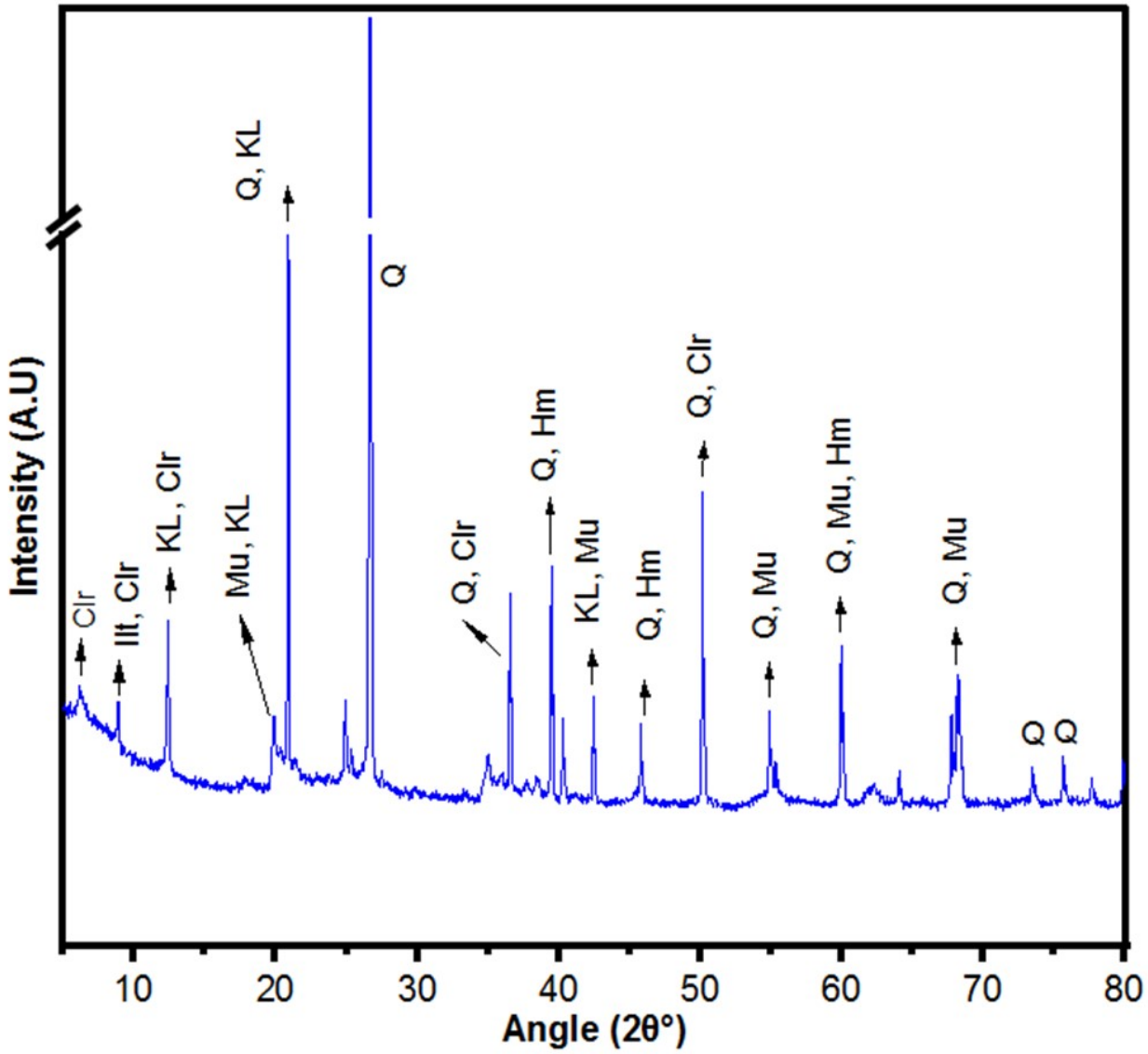

Fig. S1 XRD (Cu Kα radiation at 45kV, 40 mA) study for mineralogical investigation of the LFLS soil (Clr=Chlorite; Ilt=Illite; KL= Kaolinite; Mu= Muscovite; Q= Quartz; Hm= Haematite).

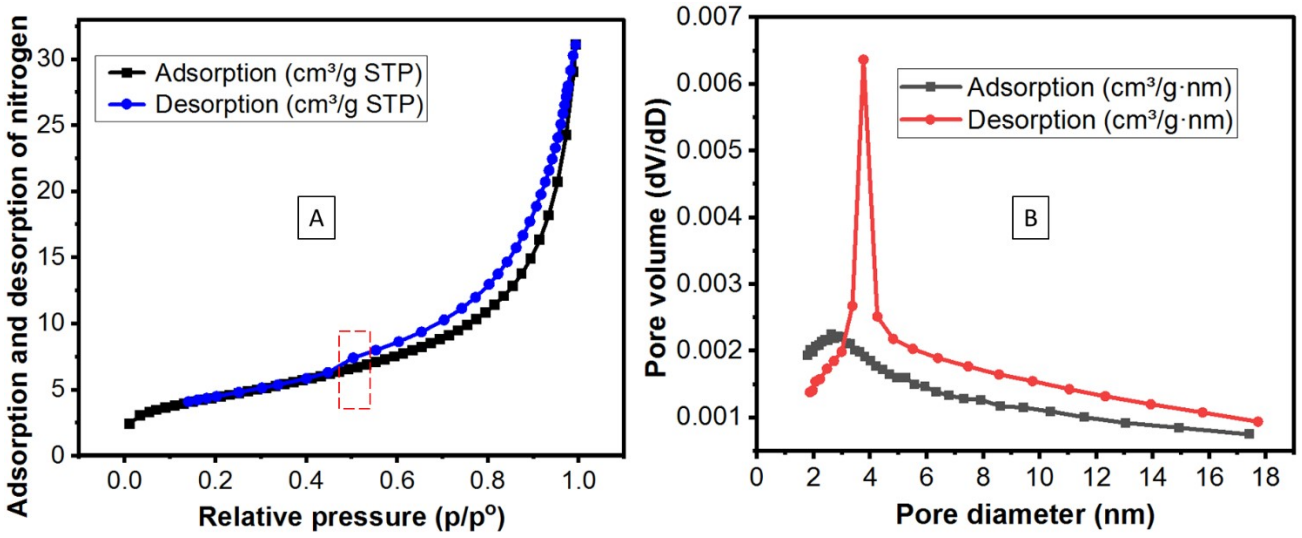

Fig. S2 Brunauer-Emmett-Teller (BET) surface area of LFLS soil. (A) Adsorption-desorption loop at $p/p^o>0.4$ represents the porous (plate slit, narrow crack, and wedge pores) structure of the soil; (B) The presence of both micro (≤2 nm) and mesopores (2-50 nm) were also confirmed by the 1.79-17.4 nm pore diameter. Adsorption-desorption isotherm of nitrogen gas indicates single layer adsorption at low pressure (mesopore filling), and then multilayer adsorption and capillary condensation at high pressure (micropore filling) [10, 11].

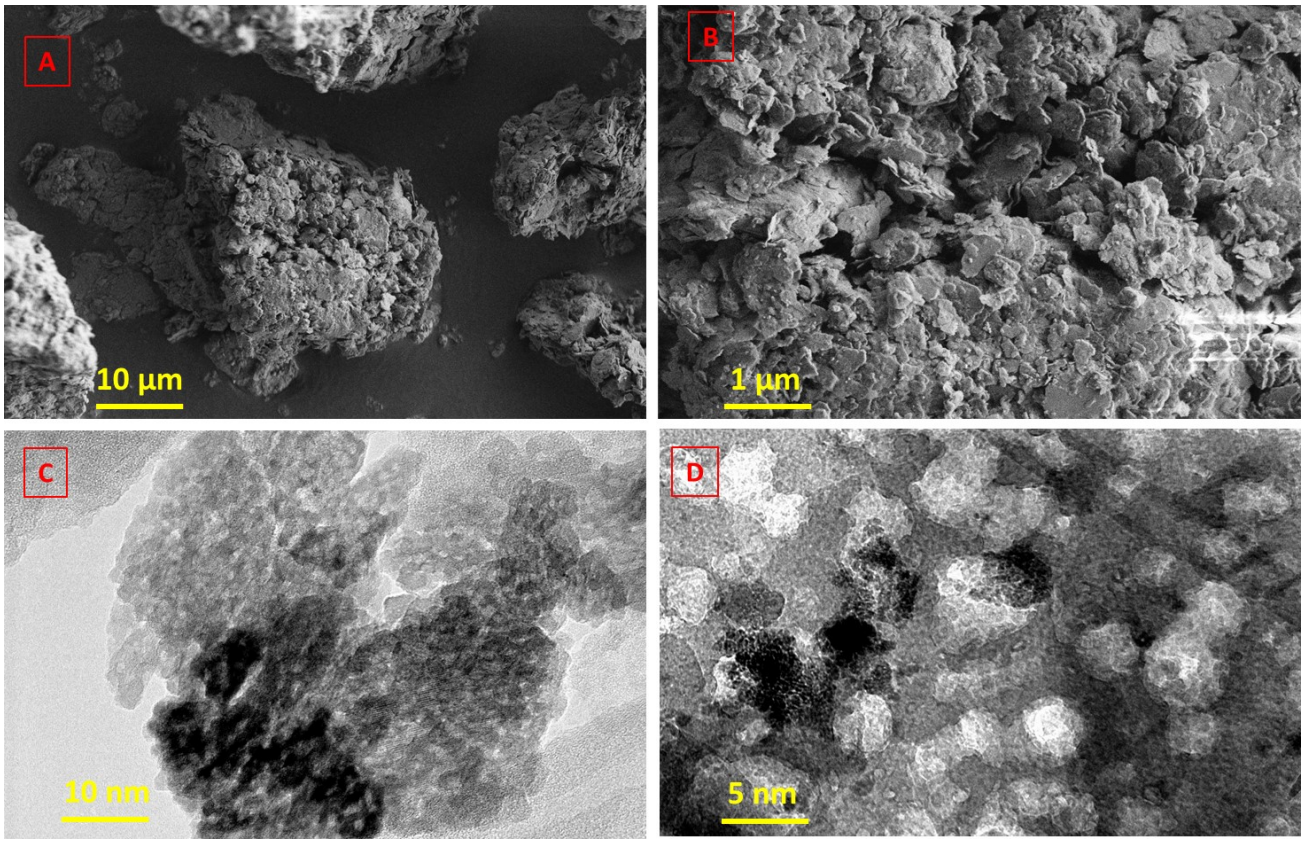

Fig. S3 Surface morphology of the studied soil. (A, B) Scanning Electron Microscope (SEM) represents agglomerated particles resulting in the porosity on the soil surface; (C, D) Transition Electron Microscope (TEM) indicates both meso and mico pore present in the soil structure.

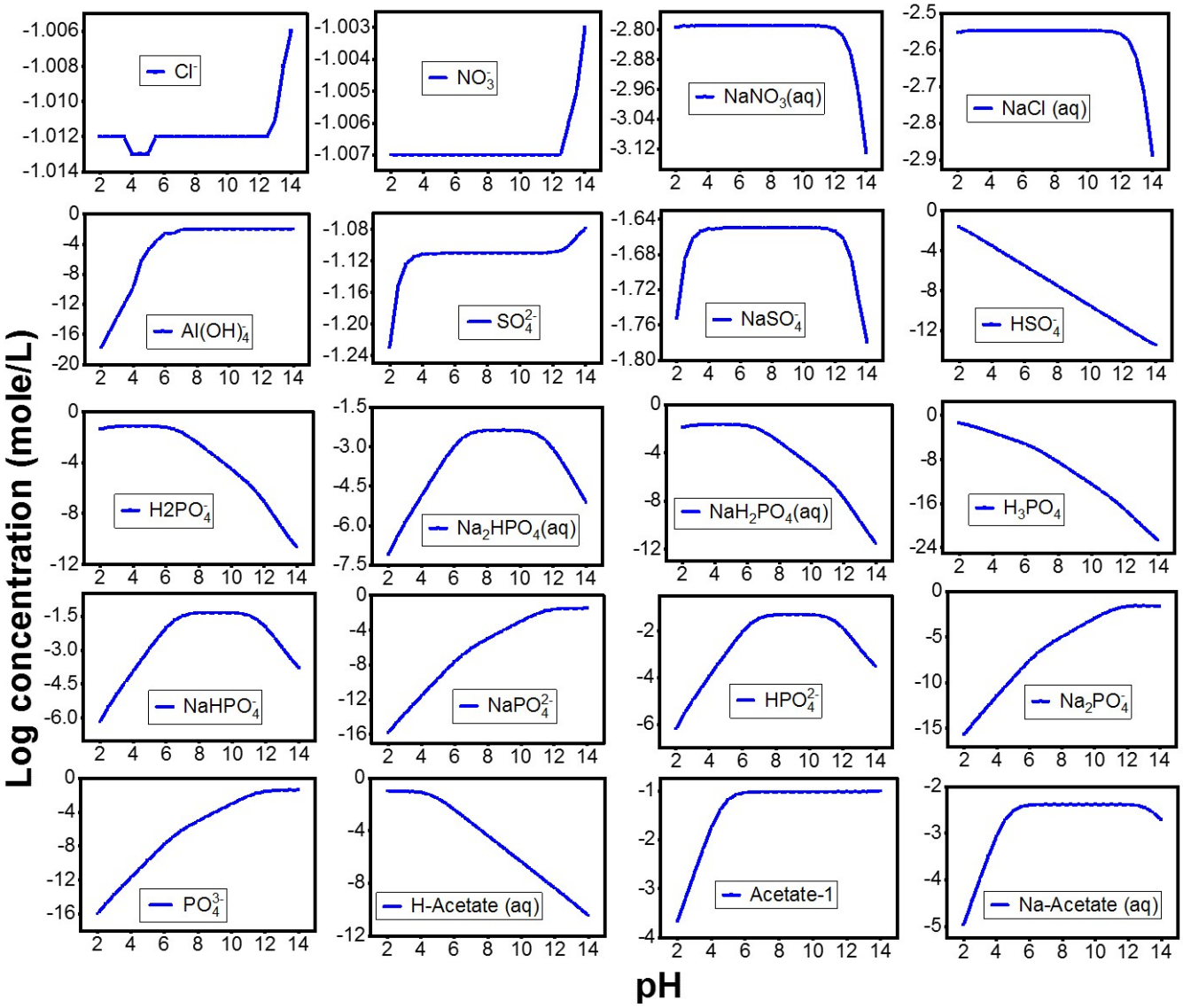

Fig. S4 Different anions and species in aqueous solution (obtained using visual MITEQ simulation) reflect their solubility and potential interaction with Be under different pH levels.

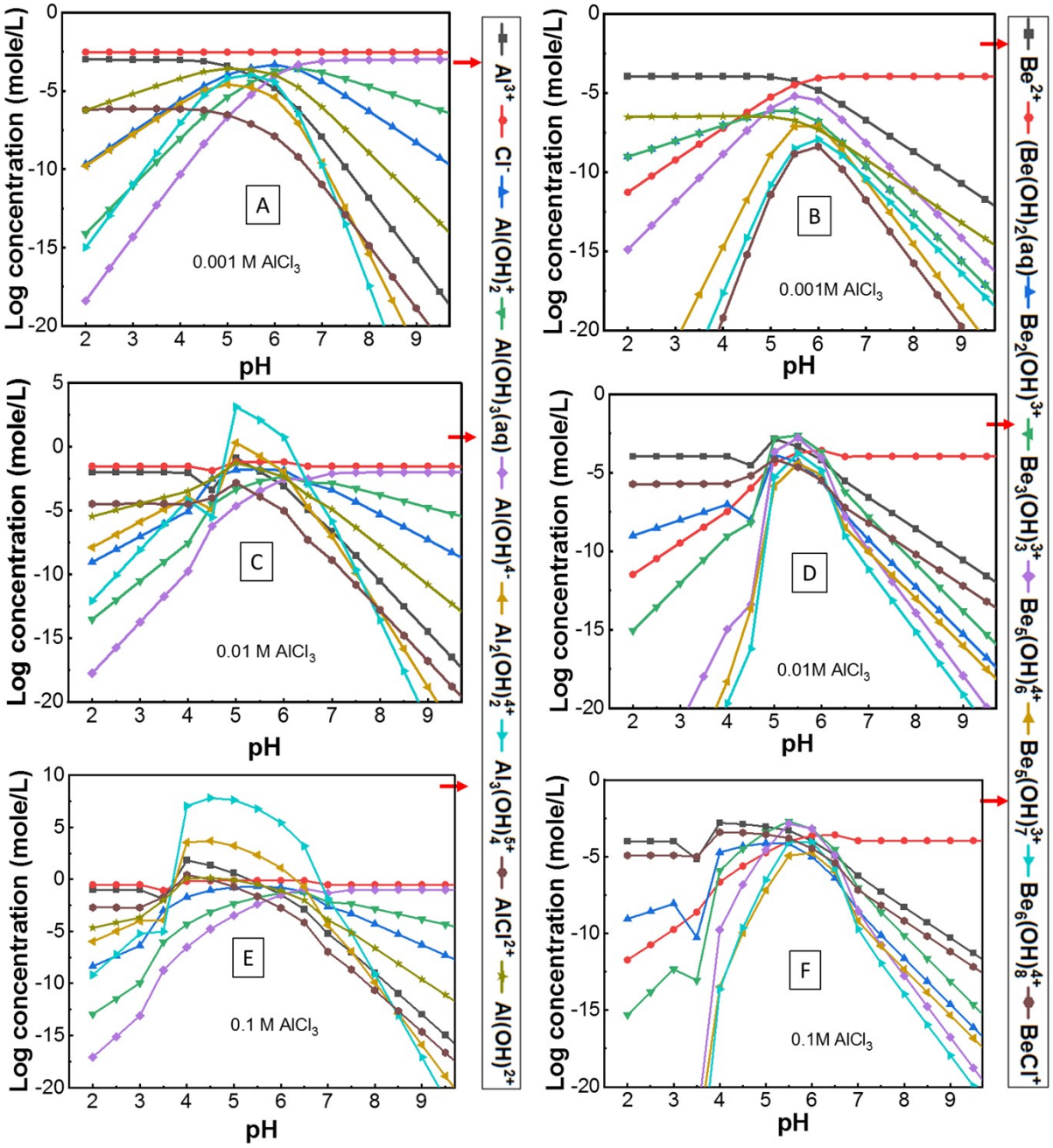

Fig. S5 Effect of $AlCl_3$ concentration (0.001-0.1M) on different species of aluminium and Be in solution (data from visual MINTEQ 3.1). (A, B) At 0.001M $AlCl_3$, the positive hydrolysis products of both Al and Be were increased up to pH 6 and then decreased smoothly; (C, D) A decline in the amounts of each species was found at pH 4.5 while considering 0.01M $AlCl_3$ solution; (E, F) Reduction in the species was mainly noticed for 0.1 M $AlCl_3$ solution at pH 3.5. From this simulation data, it is noted that the concentration of $AlCl_3$ shows significant effects on the solubility, hydrolysis species and sorption-desorption phenomena of Al and Be. However, a higher concentration (e.g. <0.01M $AlCl_3$) may not be applicable for visual

MINTEQ simulation since it suggests the number of interactions might reach the maximum allowable concentration as specified in the database file.

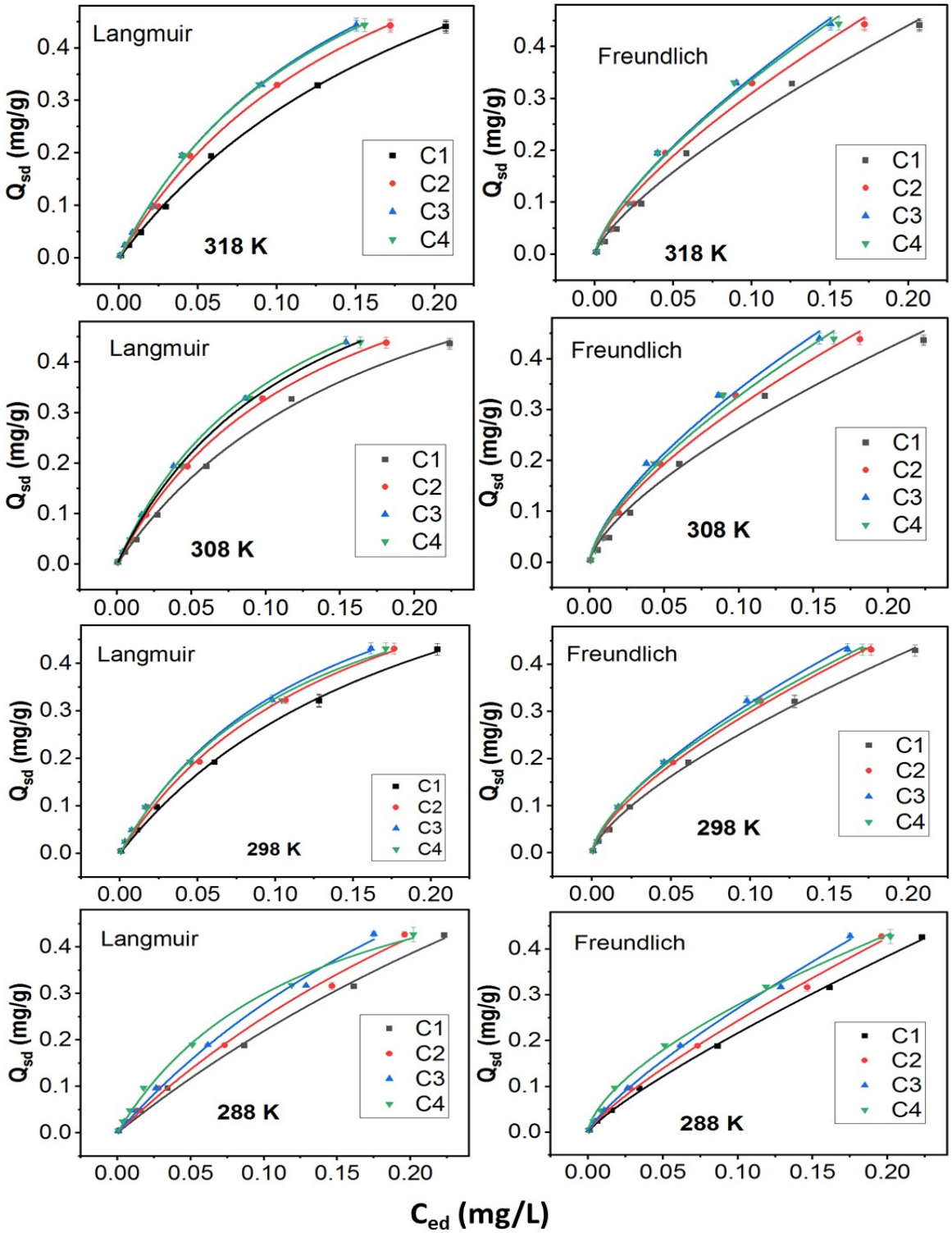

Fig. S6 Langmuir and Freundlich desorption isotherm models at different temperatures and desorption cycles. Q_{sd} represents the amount of Be present in the solid surface (still sorbed) after each desorption cycle.

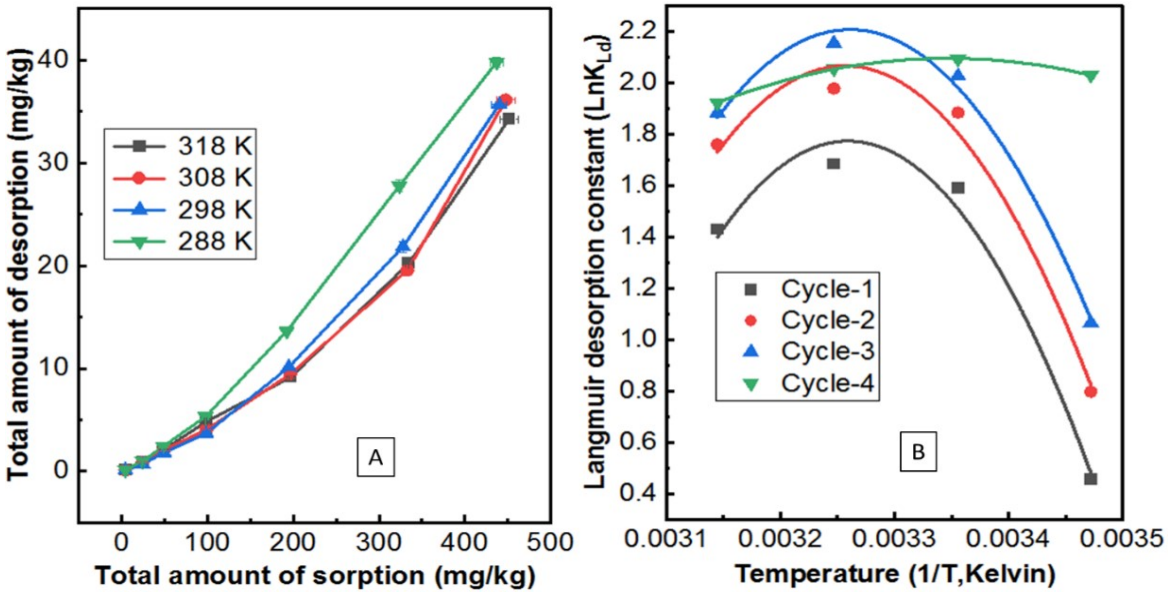

Fig. S7 (A) Effect of temperature on total desorption (C1+C2+C3+C4) of Be from the sorbed amount; (B) Non-linear dependence of Langmuir desorption constant on temperature.

References

1. T. E. Payne, Little Forest Legacy Site – Summary of site history until the commencement of waste disposal in 1960; Report no.ANSTO / E-782; ANSTO Institute for Environmental Research, 2015.
2. D. Cendón, C. Hughes, J. Harrison, S. Hankin, M. Johansen, T. Payne, H. Wong, B. Rowling, M. Vine and K. Wilsher, Identification of sources and processes in a low-level radioactive waste site adjacent to landfills: groundwater hydrogeochemistry and isotopes, *Australian Journal of Earth Sciences*, 2015, **62**, 123-141.
3. T. Payne, Background report on the Little Forest Burial Ground legacy waste site (ANSTO/E-780). Lucas Heights, NSW: Australian Nuclear Science and Technology Organisation, 2012.
4. T. E. Payne, J. J. Harrison, C. E. Hughes, M. P. Johansen, S. Thiruvoth, K. L. Wilsher, D. I. Cendón, S. I. Hankin, B. Rowling and A. Zawadzki, Trench 'bathtubbing'and surface plutonium contamination at a legacy radioactive waste site, *Environmental science & technology*, 2013, **47**, 13284-13293.
5. K. Li, L. Qian, X. Li, Y. Ma and W. Zhou, BeO Utilization in Reactors for the Improvement of Extreme Reactor Environments-A Review, *Frontiers in Energy Research*, 2021, 214.
6. P. Bonhote, *Possible concentration and disposal processes for low level treatmen plant sludge*, Australian Atomic Energy Commission Research Establishment (AAEC), 1964.

7. M. R. Islam, P. Sanderson, M. P. Johansen, T. E. Payne and R. Naidu, The influence of soil properties on sorption-desorption of beryllium at a low level radioactive legacy waste site, *Chemosphere*, 2021, **268**, 129338.
8. G. Rayment and F. R. Higginson, *Australian laboratory handbook of soil and water chemical methods*, Inkata Press Pty Ltd, 1992.
9. U. Ilstedt, A. Nordgren and A. Malmer, Optimum soil water for soil respiration before and after amendment with glucose in humid tropical acrisols and a boreal mor layer, *Soil Biology and Biochemistry*, 2000, **32**, 1591-1599.
10. S. Fu, Q. Fang, A. Li, Z. Li, J. Han, X. Dang and W. Han, Accurate characterization of full pore size distribution of tight sandstones by low-temperature nitrogen gas adsorption and high-pressure mercury intrusion combination method, *Energy Science & Engineering*, 2021, **9**, 80-100.
11. L. Qi, X. Tang, Z. Wang and X. Peng, Pore characterization of different types of coal from coal and gas outburst disaster sites using low temperature nitrogen adsorption approach, *International Journal of Mining Science and Technology*, 2017, **27**, 371-377.